J. Fluid Mech. (1993), *vol.* 246, *pp.* 117–141

Nonlinear and free-surface effects on the spin-down of barotropic axisymmetric vortices

By LEO R. M. MAAS

Netherlands Institute for Sea Research, P.O. Box 59, 1790 AB Den Burg, The Netherlands

(Received 17 January 1992 and in revised form 29 June 1992)

The spin-down of a barotropic axisymmetric vortex, such as observed in laboratory models, is examined analytically. In addition to the classical, self-similar Ekman decay due to viscous effects (Greenspan & Howard 1963), which is characterized by an azimuthal velocity profile with the position of its maximum velocity fixed and a decay time equal to the Ekman timescale, the effects of nonlinearity and a free surface are considered separately.

The Ekman circulation in the radial and vertical planes whose strength is determined by the vorticity of the overlying fluid, leads to radial advection of the azimuthal velocity. This nonlinearity results in a nonlinear kinematic wave equation for the circulation and leads to the outward/inward propagation of the position of maximum azimuthal velocity for cyclonic/anticyclonic vortices. The associated steepening of the azimuthal velocity profile may lead to a shock formation when the absolute vorticity of the initial profile is negative at a certain radius. For anticyclonic vortices having a monotonically increasing angular velocity profile this shock formation occurs at the core. For such vortices (or arbitrary cyclonic vortices) this dynamical 'breaking' criterion is, despite significant differences in the physics concerned, identical to Rayleigh's kinematical criterion for the onset of centrifugal instability.

For a dynamically active free-surface fluid the spin-down of a decaying vortex is prolonged by a radially dependent factor proportional to the Froude number. This conclusion holds both in a cylinder with a parabolic bottom (mimicking the shape of the free surface of a fluid in solid-body rotation) and in a flat-bottomed cylinder. In view of the constancy of background vorticity the former geometry is relevant for a comparison to geophysical f-plane vortices. The latter geometry, however, is more easily established in a laboratory experiment, but the evolution of the azimuthal velocity profile is much more complicated and depends on the initial azimuthal velocity profile in a highly convoluted way.

1. Introduction

The evolution of axisymmetric vortices in a rotating tank, filled with a homogeneous fluid, can be considered as a generalized spin-up, or spin-down problem. In the remainder of this paper we will refer to the decay of vortices relative to the solid-body, background flow always as a *spin-down* process, although, technically, one should distinguish between spin-up and spin-down for anticyclonic and cyclonic vortices respectively; a distinction that will be touched upon when discussing the difference in stability properties between the two (see §3).

In the classical spin-up problem (described in Greenspan 1968 and Benton & Clark 1974) it is natural to suppose that the fluid, adjusting itself to a (nearly) impulsive

change in angular velocity of the tank, is initially in a state of solid-body rotation (having a uniform vorticity profile), which may be the state of no-motion, as when the fluid is spun-up from rest. More general initial states, in which the vorticity profile is non-uniform, may be created by alternative 'procedures', in which it is not the tank whose angular velocity is changed, but in which the fluid acquires a radially dependent angular velocity. These procedures are described in the experimental studies of Kloosterziel (1990) and Kloosterziel & van Heijst (1992), and consist of ways in which barotropic vortices can be created in a rotating tank filled with a homogenous fluid by raising an inner cylinder, which is filled with a similar fluid (of the same density). The fluid in this inner cylinder has been given a larger or smaller angular velocity, either by stirring (creating so-called *stirring* vortices), or by raising, or lowering the depth of the fluid in the inner cylinder (resulting in so-called *collapse* vortices). An alternative, third way consists of adding or withdrawing fluid (leading to so-called *sink* vortices). It is observed that the motion rapidly becomes two-dimensional and often axisymmetric (Kloosterziel & van Heijst 1992). Under certain conditions, non-axisymmetric di- and tripoles are formed directly in the initial phase (Kloosterziel & van Heijst 1991; van Heijst, Kloosterziel & Williams 1991). These fall outside the scope of the present paper. Instabilities of axisymmetric vortices, however, will briefly be discussed in §3. The axisymmetrization of stable elliptical vortices appears to be a robust feature of the Euler equations (Melander, McWilliams & Zabusky 1987) and may perhaps be operating similarly in the rotating tank at the initial, nondescript phase leading to the circularly symmetric 'initial' states observed, whose evolution in the subsequent spin-down process is considered here.

In spin-up studies (e.g. Greenspan & Howard 1963 and Wedemeyer 1964) angular momentum is imparted to, or withdrawn from the fluid in two ways: either by friction at the sidewall and subsequent diffusion inwards, characterized by a diffusive timescale $T_d \equiv L^2/\nu$ (where L is the vortex scale and ν the kinematic viscosity); or at the bottom (and, when rigid, surface), which is driving the convective, secondary Ekman circulation, characterized by the Ekman timescale $T_E \equiv \Omega_0^{-1} E^{-\frac{1}{2}}$ (where Ω_0 is the angular velocity of the rotating tank and $E \equiv \nu/\Omega_0 H^2$ is the Ekman number, in which H denotes a depth scale). The relative importance of these two processes is measured by the ratio of their timescales: $T_E/T_d = E^{\frac{1}{2}}(H/L)^2$ (Watkins & Hussey 1977). For $H/L \leqslant O(1)$, this ratio is small for what is (geo)physically the most interesting situation, i.e. $E \ll 1$, corresponding to a rapidly rotating fluid. Therefore it is the Ekman circulation which is determining the evolution of the vortices.

The Ekman circulation may affect the evolution of the vortex in the interior region (i.e. away from frictional boundary layers) in two ways. First, it acts as a sink or source of vorticity, through the compression or stretching of background (in geophysical applications termed 'planetary') vortex tubes. Secondly, it may contribute directly to the advection of azimuthal momentum – a nonlinear feature.

The Rossby number, ϵ, determines the importance of this nonlinearity. In the classical spin-up context it is defined as the ratio of the difference in angular velocities of the fluid and the tank, $\Delta\Omega$, and the angular velocity of the tank, Ω_0: $\epsilon = \Delta\Omega/\Omega_0$. In the present generalized spin-down context it is defined as the ratio of the relative angular velocity scale U/L (where U denotes the scale of the azimuthal velocity field, which is negative for anticyclonic vortices) and the angular velocity of the tank Ω_0: $\epsilon = U/\Omega_0 L$. For small values of the Rossby number ($|\epsilon| \ll 1$) the Ekman suction velocity is linearly related to the vorticity of the fluid in the interior directly overlying it (i.e. of the fluid at the same radial position) (Greenspan 1968). For two reasons this is no longer true for $|\epsilon| = O(1)$. First, the Ekman suction velocity then

becomes nonlinearly related to the vorticity of the overlying fluid, as indicated by the numerical analysis of Rogers & Lance (1960) for the spin-up of a fluid above an infinite disk for arbitrary ratios of angular velocities of the fluid (at 'infinity') and the wall. Second, the local Ekman suction velocity will no longer be related to the interior vorticity field at the same location. Even though the application by Wedemeyer (1964) and Weidman (1976) of a local relation to a non-uniform angular velocity profile (such as appears during spin-up from rest in a rotating rank of finite extension) was largely successful, Benton (1979) pointed out a serious failure of this model, in that the vorticity field acquires an unphysical maximum at an intermediate radial position. However, notwithstanding Benton's criticism, the relation between the Ekman suction velocity and the interior vorticity is approximately linear over a surprisingly large interval of angular velocities (see Greenspan 1968, figure 3.4), approximately corresponding to Rossby numbers $|\epsilon| < 0.6$. It is therefore tempting to apply this same relation to describe the Ekman suction in the evolution of relatively strong vortices too, as did Kloosterziel (1990) and Kloosterziel & van Heijst (1992). The evolution equation of the azimuthal velocity profile (essentially an inviscid form of Wedemeyer's 1964 equation), which they thus derived and examined numerically, can in fact be solved analytically for an arbitrary initial velocity profile (§3). It confirms the outward (inward) propagation of the position of maximum azimuthal velocity and associated steepening for a cyclonic (anticyclonic) vortex and shows that, under certain conditions on the initial profile, this may lead to 'breaking' (i.e. multivaluedness of the azimuthal velocity profile). The remarkable result, arrived at here, is that this *dynamic* criterion for breaking is virtually equivalent to Rayleigh's (1916) *kinematic* stability criterion.

The presence of a free surface will introduce additional effects, which may lead to a widening of an initial azimuthal velocity profile (in contradistinction to the effect of nonlinearity, discussed above) and to a slow-down of the decay process of the vortex.

The importance of a deformable free surface is measured by the Froude number $F \equiv \Omega_0^2 L^2/gH$ (where g is the acceleration due to gravity). The effect of a free surface was first discussed for the classical spin-up problem, in a linear context ($|\epsilon| \ll 1$), by Greenspan & Howard (1963), who concluded that (in a flat-bottomed rotating tank) for small Froude numbers, $F \ll 1$, the fluid is spun-up as a solid body, just as in the case of a rigid surface, albeit at a slightly decreased rate. Cederlöf (1988) criticized their result, arguing that simple solid-body spin-up in this geometry was due to a cancellation of the true dynamic effect of a deformable free surface by a geometric effect caused by the false topography created by the paraboloidal equilibrium surface in a rotating flat-bottomed tank, which would also be present for a non-deformable surface of the same shape. He subsequently showed that in a cylinder having a paraboloidal bottom, exactly similar to the equilibrium free surface, the azimuthal velocity field varies quadratically with radius (rather than linearly, as in the solid-body context). The total depth of the fluid column (when at rest relative to the spinning container) in his geometry is thus a constant and can therefore perhaps better serve as a laboratory model to study the evolution of geophysical vortices on an f-plane than a flat-bottomed tank. Besides this, Cederlöf may also, less importantly, have been motivated in this choice of geometry by the fact that the partial differential equation describing the evolution of the free surface now becomes separable (as was observed by Berman, Bradford & Lundgren 1983, in a two-layer spin-up study), and is readily integrated for arbitrary values of the Froude number. In this way he was able to establish the increase of the spin-up timescale by a factor

which, depending on radial position, is $O(F)$. His analysis can be amended to study the evolution of an arbitrary initial vortex profile in a parabolic container as we will see in §4.

Kloosterziel (1990), Kloosterziel & van Heijst (1992) and O'Donnell & Linden (1991) independently observed (and the latter authors verified experimentally) that for linear ($|\epsilon| \ll 1$) spin-up in a flat-bottomed tank the timescale is also increased by a factor proportional to F, irrespective of its value. However, in contrast to the radial dependence of the spin-up timescale in the parabolic geometry, the fluid still spins-up as a solid body and this therefore extends the small-Froude-number result of Greenspan & Howard (1963) to arbitrary Froude numbers.

In §4 it will be shown that for the flat-bottomed tank also the generalized spin-down problem – in this linear ($|\epsilon| \ll 1$) context – can be described in analytical terms; i.e. the evolution of an arbitrary initial azimuthal velocity field can be obtained in a closed form for arbitrary values of the Froude number, corroborating numerical results by Kloosterziel (1990) and Kloosterziel & van Heijst (1992) and showing, specifically, the widening of the initial velocity profile, the increase in decay time and the outward propagation of the position of maximum azimuthal velocity.

The only study allowing simultaneously for nonlinear ($|\epsilon| = O(1)$) and free-surface effects ($F = O(1)$) is by Goller & Ranov (1968), who studied the spin-up from rest of a free-surface fluid numerically. They showed that spin-up is again delayed, due to free-surface effects, in proportionality with the Froude number. This situation does not seem to be analytically tractable and is not further discussed here.

2. Governing equations

The axisymmetric flow of a homogeneous fluid in a cylinder rotating with angular frequency Ω_0 about the axis of symmetry (the z-axis), which is aligned with the gravitational acceleration direction, is, in cylindrical coordinates (r, θ, z), given by the equations of motion:

$$\frac{\mathrm{d}u}{\mathrm{d}t} - \frac{v^2}{r} - 2\Omega_0 v = -\frac{1}{\rho}\frac{\partial p}{\partial r} + \Omega_0^2 r + \nu \frac{\partial}{\partial r}\left(\frac{1}{r}\frac{\partial}{\partial r}(ru)\right) + \nu \frac{\partial^2 u}{\partial z^2}, \tag{2.1a}$$

$$\frac{\mathrm{d}v}{\mathrm{d}t} + \frac{uv}{r} + 2\Omega_0 u = \nu \frac{\partial}{\partial r}\left(\frac{1}{r}\frac{\partial}{\partial r}(rv)\right) + \nu \frac{\partial^2 v}{\partial z^2}, \tag{2.1b}$$

$$\frac{\mathrm{d}w}{\mathrm{d}t} = -\frac{1}{\rho}\frac{\partial p}{\partial z} - g + \frac{\nu}{r}\left(\frac{\partial}{\partial r} r \frac{\partial w}{\partial r}\right) + \nu \frac{\partial^2 w}{\partial z^2}, \tag{2.1c}$$

and continuity equation

$$\frac{\partial w}{\partial z} + \frac{1}{r}\frac{\partial}{\partial r}(ru) = 0. \tag{2.1d}$$

The total derivative is defined as

$$\frac{\mathrm{d}}{\mathrm{d}t} = \frac{\partial}{\partial t} + u\frac{\partial}{\partial r} + w\frac{\partial}{\partial z}.$$

Here u, v and w denote the radial, azimuthal and axial velocity components respectively; ρ is the uniform density of the fluid; ν the kinematic viscosity and g the acceleration due to gravity. The pressure, p, in the uniformly rotating frame of reference, is given as the sum of (i) a reference pressure, $\rho g H$, set by the centre depth,

H, of the uniformly rotating fluid, (ii) a hydrostatic part, $-\rho gz$, (iii) the pressure field associated with the parabolic shape of the free-surface, which it acquires when the fluid is at rest relative to the rotating frame, $\frac{1}{2}\rho\Omega_0^2 r^2$, and (iv) the time-dependent part associated with the vortex, $p'(r,z,t)$:

$$p(r,z,t) = \rho g(H-z)+\tfrac{1}{2}\rho\Omega_0^2 r^2+p'(r,z,t). \tag{2.2}$$

The fluid is confined to a region

$$0 \leqslant r \leqslant R, \tag{2.3a}$$

$$z_0(r) \leqslant z \leqslant z_s \equiv H+\Omega_0^2 r^2/2g+\eta(r,t), \tag{2.3b}$$

R being the radius of the tank and $z_s(r,t)$ is the position of the free surface, in which $\eta(r,t)$ is the time-dependent part associated with the decaying vortex. The bottom of the tank is given by the circularly symmetric profile $z_0(r)$, which, in the following, will either be flat ($z_0 = 0$), or equal to the equilibrium parabolic profile ($z_0(r) = \Omega_0^2 r^2/2g$). These equations are non-dimensionalized by use of the following scales (denoted by brackets):

$$[u,v,w,p,\eta] = U[E^{\frac{1}{2}}, 1, E^{\frac{1}{2}}\delta, \rho\Omega_0 L, \Omega_0 L/g], \tag{2.4a}$$

and

$$[r,z,t] = [L, H, E^{-\frac{1}{2}}\Omega_0^{-1}], \tag{2.4b}$$

in which the dimensionless Ekman number, $E \equiv \nu/\Omega_0 H^2$ and aspect ratio, $\delta \equiv H/L$, appear, and L and U refer to the vortex length and velocity scales respectively. With this choice we acknowledge *a priori* that for small Ekman numbers ($E \ll 1$, the situation we will consider throughout) the circulation is primarily azimuthal, while the radial circulation, driven by friction in the Ekman layer, enters only at $O(E^{\frac{1}{2}})$. This implies that the time over which the decay of the initial profile proceeds is also prolonged, compared to the rotation period, by a factor $E^{-\frac{1}{2}}$, so that time is scaled with the Ekman timescale $E^{-\frac{1}{2}}\Omega_0^{-1}$.

With these scalings (2.1) become (using the same symbols, now understood to be non-dimensionalized according to the scheme in (2.4))

$$E\left(\frac{\partial u}{\partial t}+\epsilon\left(u\frac{\partial u}{\partial r}+w\frac{\partial u}{\partial z}\right)\right)-\epsilon\frac{v^2}{r}-2v = -\frac{\partial p}{\partial r}+\frac{1}{\epsilon}r+E^{\frac{3}{2}}\left(\frac{\partial}{\partial r}\frac{\delta^2}{r}\frac{\partial}{\partial r}(ru)+\frac{\partial^2 u}{\partial z^2}\right), \tag{2.5a}$$

$$\frac{\partial v}{\partial t}+\epsilon\left(u\frac{\partial v}{\partial r}+w\frac{\partial v}{\partial z}+\frac{uv}{r}\right)+2u = E^{\frac{1}{2}}\left(\frac{\partial}{\partial r}\frac{\delta^2}{r}\frac{\partial}{\partial r}(rv)+\frac{\partial^2 v}{\partial z^2}\right), \tag{2.5b}$$

$$E\delta^2\epsilon F\left(\frac{\partial w}{\partial t}+\epsilon\left(u\frac{\partial w}{\partial r}+w\frac{\partial w}{\partial z}\right)\right) = -\epsilon F\frac{\partial p}{\partial z}-1+\delta^2 E^{\frac{3}{2}}\epsilon F\left(\frac{\delta^2}{r}\frac{\partial}{\partial r}\left(r\frac{\partial w}{\partial r}\right)+\frac{\partial^2 w}{\partial z^2}\right), \tag{2.5c}$$

$$\frac{\partial w}{\partial z}+\frac{1}{r}\frac{\partial}{\partial r}(ru) = 0. \tag{2.5d}$$

This introduces two additional dimensionless quantities: the Rossby number $\epsilon \equiv U/\Omega_0 L$ and the Froude number $F \equiv \Omega_0^2 L^2/gH$. The non-dimensional pressure (2.2) is given by

$$p = (1-z+\tfrac{1}{2}Fr^2+\epsilon Fp')/(\epsilon F), \tag{2.6}$$

and the fluid is contained within the following non-dimensional domain:

$$0 \leqslant r \leqslant R, \tag{2.7a}$$

$$z_0 \leqslant z \leqslant z_s = 1+\tfrac{1}{2}Fr^2+\epsilon F\eta(r,t), \tag{2.7b}$$

where the dimensionless topography, $z_0(r)$, is either flat or parabolic ($\frac{1}{2}Fr^2$).

We can, in view of our basic assumption ($E^{\frac{1}{2}} \ll 1$) formally set up expansions in terms of this small parameter. For the present study it suffices, however, to set $E = 0$ outside boundary layers in (2.5), since, through our choice of scales, all interesting features appear at zeroth order (see Greenspan 1968 and Kloosterziel & van Heijst 1992). Employing (2.6) we then obtain

$$\epsilon\frac{v^2}{r}+2v=\frac{\partial p'}{\partial r}, \qquad \frac{\partial v}{\partial t}+\epsilon\left(u\frac{\partial v}{\partial r}+w\frac{\partial v}{\partial z}+\frac{uv}{r}\right)+2u=0, \tag{2.8a, b}$$

$$\frac{\partial p'}{\partial z}=0, \qquad \frac{\partial w}{\partial z}+\frac{1}{r}\frac{\partial}{\partial r}(ru)=0. \tag{2.8c, d}$$

Equation (2.8c) expresses hydrostacy, which implies

$$p'(r,z,t)=\eta(r,t) \quad \text{and} \quad \frac{\partial u}{\partial z}=\frac{\partial v}{\partial z}=0, \tag{2.9a, b}$$

vertically uniform pressure and horizontal velocity fields. The continuity equation, then, can be vertically integrated. The vertical velocity at the bottom, however, is not only given by the geometrically induced component, $u\,\partial z_0/\partial r$, but also by the Ekman pumping velocity, w_E, at the top of the bottom Ekman layer (see the Appendix).

Thus, the final equations describing the evolution of the vortex due to nonlinear and free-surface effects are given by

$$\epsilon\frac{v^2}{r}+2v=\frac{\partial \eta}{\partial r}, \qquad \frac{\partial v}{\partial t}+2u\left(\frac{\epsilon}{2r}\frac{\partial}{\partial r}(rv)+1\right)=0, \tag{2.10a, b}$$

$$F\frac{\partial \eta}{\partial t}+\frac{1}{r}\frac{\partial}{\partial r}(ru\,(1+\tfrac{1}{2}Fr^2+\epsilon F\eta-z_0))=w_E, \tag{2.10c}$$

with the Ekman pump velocity, w_E given by (A 4) and (A 5) to zeroth and first order in the Rossby number respectively and the bottom profile, z_0 by 0 or $\frac{1}{2}Fr^2$. The prescribed initial condition is given by $v(r,0)=v_0(r)$, which is cyclostrophically related to an initial free-surface profile by (2.10a). When both free-surface and nonlinear effects are small ($F \ll 1$ and $\epsilon \ll 1$) equations (2.10b, c) and (A 4) directly imply the decay of the initial profile (Greenspan & Howard 1963):

$$v(r,t)=v_0(r)\exp(-t).$$

The profile retains its structure, has a fixed peak position and a simple Ekman decay timescale. In §§3 and 4 we will consider the evolution of an initial vortex when nonlinear or free-surface effects come into play and see how these conclusions are modified.

3. Vortex evolution due to nonlinear Ekman circulation ($F \ll 1$)

When the Froude number is small ($F \ll 1$) the surface is rigid insofar that it does not directly respond to the vertical Ekman pumping at the top of the bottom boundary layer. This mass flux then is entirely turned into a radial mass flux. For analytical purposes it will be convenient to first exploit the classical Ekman pumping law (A 4), which relates the local Ekman pumping velocity to the local interior

vorticity in a linear way. The resulting evolution for the azimuthal velocity in the interior can then be evaluated exactly (§3.1). Its formal limitation ($\epsilon \ll 1$) will require us subsequently to consider the effect of an improved Ekman pumping velocity, as given by the combination of (A 4) and (A 5), (§3.2).

3.1. *Linear Ekman pumping*

Inserting (A 4) into (2.10*c*), setting $F = 0$, we find the radial velocity to be equal to half the azimuthal velocity of the interior. (Note that the azimuthal velocity at the top of the boundary layer, denoted as v_∞ in the Appendix, is identical to the interior azimuthal velocity, v, as used in (2.10)). Inserting this in (2.10*b*) the evolution of the azimuthal velocity is, as noted by Kloosterziel & van Heijst (1992), given by an inviscid form of Wedemeyer's (1964) equation:

$$\frac{\partial v}{\partial t} + v\left(\frac{\epsilon}{2r}\frac{\partial}{\partial r}(rv) + 1\right) = 0, \qquad v(r,0) = v_0(r). \tag{3.1a, b}$$

In terms of the (scaled) circulation,

$$\Gamma \equiv \tfrac{1}{2}\epsilon r v, \tag{3.2a}$$

and radial coordinate

$$s \equiv \tfrac{1}{2}r^2, \tag{3.2b}$$

this equation takes the form

$$\frac{\partial \Gamma}{\partial t} + \Gamma\frac{\partial \Gamma}{\partial s} = -\Gamma, \qquad \Gamma(s,0) = \Gamma_0(s) \equiv \tfrac{1}{2}\epsilon(2s)^{\frac{1}{2}} v_0((2s)^{\frac{1}{2}}). \tag{3.3a, b}$$

This is a standard nonlinear hyperbolic equation, the kinematic wave equation (Whitham 1974, p. 62), describing nonlinearly propagating waves. In this case it is the peak in the azimuthal velocity profile that is propagating. Equation (3.3*a*) states that the circulation is simply exponentially decaying,

$$\mathrm{d}\Gamma/\mathrm{d}t = -\Gamma, \tag{3.4a}$$

on curves – the characteristics – determined by

$$\mathrm{d}s/\mathrm{d}t = \Gamma. \tag{3.4b}$$

Thus we obtain the exact solution for arbitrary initial profiles, $\Gamma(s,0) = \Gamma_0(s)$, in implicit form as

$$\Gamma(\xi,t) = \Gamma_0(\xi)\,\mathrm{e}^{-t}, \tag{3.5a}$$

at curves

$$s(\xi,t) = \xi + \Gamma_0(\xi)\,(1-\mathrm{e}^{-t}). \tag{3.5b}$$

This yields a parametric relation $\Gamma(s,t)$ by elimination of the parameter ξ, which is the initial position: $\xi = s(\xi,0)$.

Example 1: The Rankine vortex

The highly idealized model of a vortex having a core which is in solid-body rotation and an irrotational exterior, the Rankine vortex, is perhaps physically unrealistic, but offers the only example for which the evolution (both due to nonlinear and free-surface effects) can be made explicit. Thus, let the initial azimuthal velocity profile of the vortex be given by

$$v_0(r) = \begin{cases} r, & r \leqslant 1 \\ 1/\mathrm{r}, & 1 \leqslant r \leqslant R, \end{cases} \tag{3.6}$$

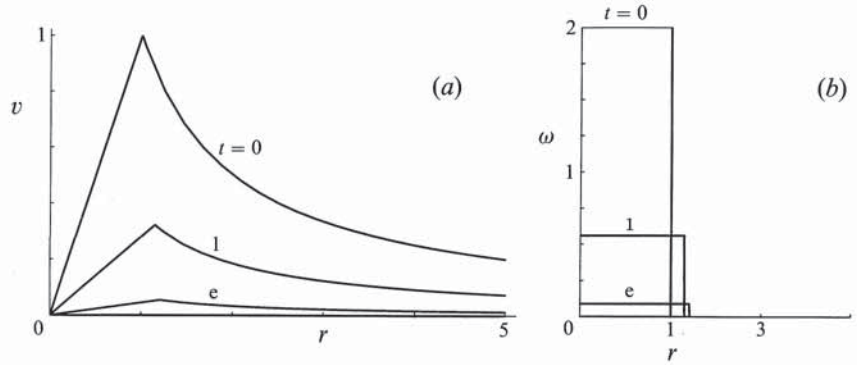

FIGURE 1. Evolution of a cyclonic Rankine vortex with $\epsilon = \frac{1}{2}$ during spin-down due to Ekman circulation. (*a*) Azimuthal velocity and (*b*) vorticity profile at successive instances of time, t.

in which R is the dimensionless tank radius (given in terms of the initial vortex scale L); then

$$v(r,t) = \begin{cases} r\,\mathrm{e}^{-t}/[1+\epsilon(1-\mathrm{e}^{-t})], & r \leqslant r_*(t), \\ (1/r)\,\mathrm{e}^{-t}, & r \geqslant r_*(t), \end{cases} \tag{3.7}$$

where the position of the peak velocity is given by

$$r_*(t) = [1+\epsilon(1-\mathrm{e}^{-t})]^{\frac{1}{2}}, \tag{3.8}$$

which therefore propagates away from its initial radius at $r_* = 1$ to its ultimate radial position at $r_* = (1+\epsilon)^{\frac{1}{2}}$. Equation (3.7) shows that the velocity profile nevertheless retains its structure so that the vorticity remains concentrated in the widening ($\epsilon > 0$), or narrowing ($\epsilon < 0$) core, while simultaneously decaying:

$$\omega \equiv \frac{1}{r}\frac{\partial}{\partial r}(rv) = \begin{cases} 2\,\mathrm{e}^{-t}/[1+\epsilon(1-\mathrm{e}^{-t})], & r \leqslant r_*(t), \\ 0, & r \geqslant r_*(t), \end{cases} \tag{3.9}$$

see figure 1.

Example 2: Two smooth vortex profiles

Kloosterziel (1990) observed that the diffusion equation on the infinite interval can be solved by a one-parameter (α) family of self-similar profiles, which offer a good diagnostic set to qualify observed vortex profiles. The two extremes, $\alpha = 1$ and $\alpha = 3$, reached by the vortices in the laboratory experiments, correspond to two profiles more commonly met in literature. The $\alpha = 1$ profile, the Lamb vortex (Saffman & Baker 1979),

$$v_0(r) = (A/r)\,(1-\exp(-r^2/B)), \tag{3.10}$$

with $A = 1.398\ldots$ and $B = 0.796\ldots$ has a vorticity profile, which, for a cyclonic vortex, is entirely positive. In a typical laboratory experiment the initial vortex profile can be typified by a value of α somewhere in between 1 and 3, while its subsequent state moves to one that can be described by $\alpha = 3$, the Gaussian vortex (whose stream function is Gaussian), with a velocity profile given by

$$v_0(r) = r\exp(\tfrac{1}{2}(1-r^2)). \tag{3.11}$$

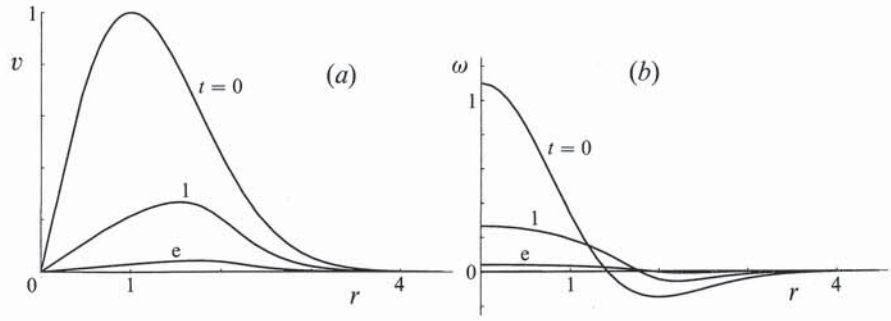

FIGURE 2. As figure 1 but for a cyclonic Gaussian vortex ($\epsilon = 1.5$). Note the 'steepening' of the azimuthal velocity profile, at the 'front-side' of the propagating peak.

Note that the amplitudes of these two velocity fields are chosen such that $v_0(1) = 1$, so as to comply with the adopted scaling. In these cases the relation for $v(r,t)$ cannot be made explicit, but the parametric relation (3.5) can be directly used to obtain the evolution as given in figure 2.

It is well-known that the evolving profile, 'propagating' in the radial direction, may exhibit breaking, i.e. multivaluedness. This occurs when two characteristics cross each other (Whitham 1974, p. 22): two neighbouring characteristics, originating from different initial positions ξ, then occupy the same position in the (s,t)-plane, so that

$$\mathrm{d}s/\mathrm{d}\xi = 0,$$

or, from (3.5*b*), when

$$1 + \Gamma_0'(\xi)\,(1 - \mathrm{e}^{-t}) = 0, \tag{3.12}$$

where the prime designates a derivative of the dependent variable. A positive time of breaking, t_B, exists only when $\Gamma_0'(\xi) < -1$, for some ξ. Conversely, there will be no breaking when

$$1 + \Gamma_0'(\xi) > 0, \quad 0 \leqslant \xi \leqslant \tfrac{1}{2}R^2,$$

in contrast to the conclusion drawn in Kloosterziel & van Heijst (1992), that every velocity profile will continue to steepen (and ultimately 'break'). In terms of the original variables, this dynamic stability requirement is translated into the condition

$$\epsilon\omega_0 + 2 \geqslant 0, \quad 0 \leqslant r \leqslant R, \tag{3.13}$$

where $\omega_0(r)$, denotes the vorticity of the initial profile: $\omega_0(r) \equiv 1/r\partial/\partial r(rv_0)$. True breaking will, of course, be inhibited by diffusive effects (neglected thus far) which may then provide the smoothing which connects the two disjoint azimuthal velocity values at either side of the shock in the case $\epsilon > 0$ (see Venezian 1970, who derived a Burgers' equation for the shock in azimuthal velocity which develops during spin-up from rest), or at the origin in the case $\epsilon < 0$. Indications of such a shock in the azimuthal velocity were present in some of the experiments of R. C. Kloosterziel (personal communication).

The examples considered above offer some insight into this stability requirement. For the *cyclonic* Rankine (equation (3.6)) and Lamb (equation (3.10)) vortex the vorticity is always positive, so that, from (3.13), these vortices will always remain stable. Only the cyclonic Gaussian vortex, (3.11), has negative vorticity lobes, outside the core, with an extreme value of $-2\mathrm{e}^{-\frac{3}{2}}$ at $r = 2$. Therefore, these vortices are stable for $\epsilon < \mathrm{e}^{\frac{3}{2}}$, see figure 3. For *anticyclonic* vortices the maximum vorticity of

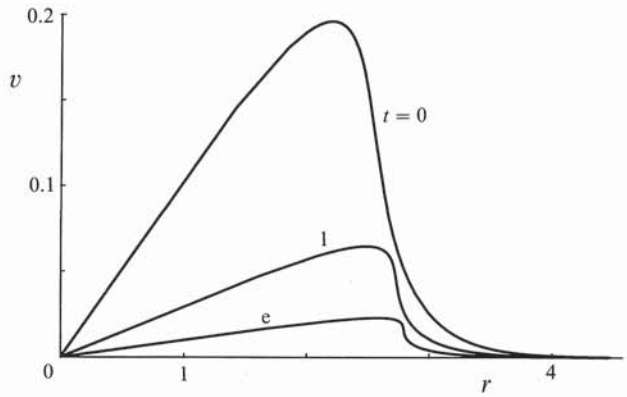

FIGURE 3. Evolution of a marginally stable cyclonic Gaussian vortex ($\epsilon = e^{\frac{3}{2}}$), i.e. which has zero absolute vorticity ($\epsilon\omega_0 + 2 = 0$).

all three profiles is at (and near) the origin, where instabilities, when occurring, first appear. The stability requirement, in this case, leads to the following conditions:

Rankine vortex: $\epsilon > -1$,

Lamb vortex: $\epsilon > -B/A \approx -0.569$,

Gaussian vortex: $\epsilon > -e^{-\frac{1}{2}} \approx -0.607$;

which are therefore more susceptible to instabilities (Kloosterziel 1990). These, and the previous requirement for the cyclonic Gaussian vortex, are all satisfied for the restrictions under which the linear Ekman pump is valid ($\epsilon \ll 1$). In the Appendix it is argued that this linear Ekman pump, however, also applies to larger values of the Rossby number, up to the stability boundaries given for the anticylonic vortices above. Indeed incorporation of the next-order Ekman pumping, considered briefly in §3.2, does not really alter this stability condition (although, in that case conclusions have to be drawn from numerical analyses).

The 'breaking' or *dynamic* stability criterion, (3.13), is remarkable since it is virtually equivalent to Rayleigh's famous *kinematical* stability criterion. This criterion states that, in an inertial frame of reference, an axisymmetric stationary flow with azimuthal velocity profile, $v_0(r)$, will be stable when the squared circulation is a monotonically increasing function of radius, i.e.

$$(\mathrm{d}/\mathrm{d}r)\,(rv_0)^2 \geqslant 0, \quad 0 \leqslant r \leqslant R. \tag{3.14}$$

Kloosterziel & van Heijst (1991) argued that, in a rotating frame of reference, this can be written as

$$(\epsilon v_0 + r)\,(\epsilon\omega_0 + 2) \geqslant 0, \quad 0 \leqslant r \leqslant R, \tag{3.15}$$

which states that the product of 'absolute velocity', $\epsilon v_0 + r$, and absolute vorticity, $\epsilon\omega_0 + 2$, should be positive. Rayleigh's (1916) result is derived by an energy argument in which two concentric fluid rings are imagined to be interchanged, while conserving their angular momentum. By comparing the kinetic energy before and after the exchange it follows that when (3.14) is satisfied the kinetic energy increases: a situation that will never be accomplished in the absence of some source of energy. Conversely, when (3.14) is not satisfied, the kinetic energy decreases: energy will become available for the unstable motions. Stability condition (3.14), or (3.15), can be obtained more rigorously by considering the stability of a perturbation of a circularly symmetric initial azimuthal velocity profile in an inviscid fluid, contained in an (or in between two) infinitely long cylinder(s), oriented parallel to the rotation

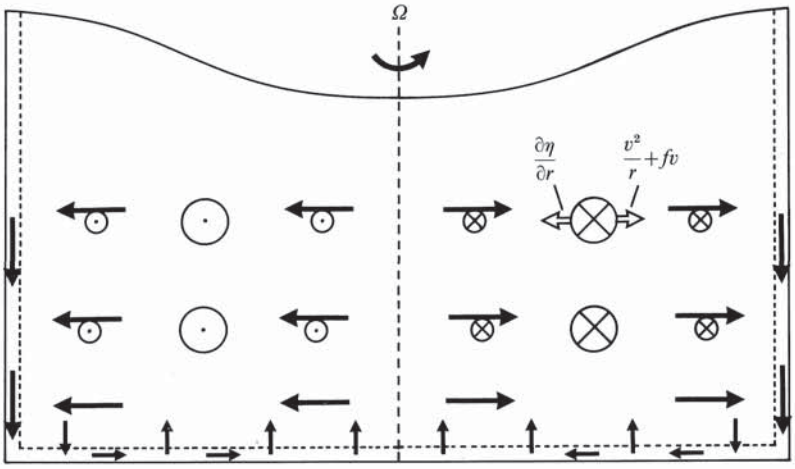

FIGURE 4. Sketch of the cross-section of the primary circulation (normal to the plane, denoted by circles) and secondary (Ekman) circulation (denoted by solid arrows) of an evolving vortex. The forces in the interior are depicted as open arrows, the inwardly directed pressure-gradient one being depth-independent and close to the bottom – where friction impedes the azimuthal flow – in excess of the Coriolis and centrifugal forces. The inwardly driven mass flux is turned into a vertical mass flux in the core of the vortex, which in turn produces a radially outward flow, which advects angular momentum outwards.

axis (Chandrasekhar 1961, p. 275). In contrast, (3.13) is obtained as the stability criterion of a finite-amplitude vortex in a shallow container of finite depth, in which viscous effects near the bottom are of predominant importance to the evolution of the inviscid interior. Physically, the stability requirement (3.13) can be explained as follows: breaking occurs when the radial gradient of azimuthal velocity and hence of relative vorticity (and in turn absolute vorticity) becomes infinitely negative. Since Ekman pumping can change only the magnitude and not the sign of the absolute vorticity, the occurrence of breaking implies that the initial absolute vorticity must have been negative somewhere. Conversely, when the initial absolute vorticity is everywhere positive, breaking cannot occur. However, despite the differences in the physical circumstances, it is striking to observe how both stability criteria practically coalesce.

In fact, under mild conditions the two are mathematically equivalent. This can be seen as follows. Condition (3.15) can, once again, be rewritten in terms of the (scaled) angular velocity

$$\Omega = \epsilon v/r, \tag{3.16}$$

as

$$2r(\Omega+1)\,(\Omega+1+\tfrac{1}{2}r\,\partial\Omega/\partial r) \geqslant 0. \tag{3.17}$$

For cyclonic vortices $\Omega > 0$ and the second factor, corresponding to (3.13), is clearly determining the stability. For anticyclonic vortices $\Omega < 0$. For the special class of vortices having a monotonically increasing angular velocity profile – a condition met with by each member of the class of profiles referred to in example 2 above; a class that fits observations of velocity profiles in the laboratory well – condition (3.15) is again entirely equivalent with the simpler (3.13). For, if $\Omega+1$ changes sign at some r (assuming that the vortex is sufficiently localized that its absolute vorticity is positive at the tank wall), the second factor in (3.17) changes sign somewhere else, because $r\partial\Omega/\partial r \geqslant 0$, thus leaving an interval of r-values where (3.15) is violated. In that case, however, the second factor in (3.17) changes sign by itself and thus (3.13)

is also violated. The two criteria, then, are identical for this class of angular velocity profiles. Note that for this restricted class of anticylonic vortices the stability criterion will be first violated at the centre of the tank.

The critical value of ϵ, derived in (3.13), now gives the Rossby number after which breaking sets in. Note that prior to this a two-dimensional instability may have started (Michalke & Timme 1967; Carton & McWilliams 1989), leading to non-axisymmetric vortices like the tripole, also observed in laboratory experiments (Kloosterziel & van Heijst 1989; van Heijst & Kloosterziel 1989; van Heijst, Kloosterziel & Williams 1991).

3.2. *Nonlinear Ekman pumping*

When Rossby numbers are not small, one needs an improvement of the zeroth-order (linear) Ekman pumping velocity, such as is obtained in a perturbative treatment of the boundary-layer dynamics. This is carried out in the Appendix, where the first-order (non-linear) Ekman pumping velocity has been calculated, (A 5). Inserting the combined vertical Ekman pumping velocity, $w_E^{(0)}+\epsilon w_E^{(1)}$, or rather the radial velocity which it implies by continuity, into (2.10*b*) yields an improved evolution equation for the azimuthal velocity. An autonomous equation like (3.3), i.e. without any explicit occurrence of the (transformed) radial coordinate, is obtained in terms of Ω, (3.16), and radial coordinate

$$\rho = \ln r^2,$$

as

$$\frac{\partial \Omega}{\partial t}+\Omega\left(1-\frac{1}{5}\Omega-\frac{7}{20}\frac{\partial \Omega}{\partial \rho}\right)\left(1+\Omega+\frac{\partial \Omega}{\partial \rho}\right)=0. \tag{3.18}$$

The need for this improved Ekman pumping was, implicitly, expressed by Kloosterziel & van Heijst (1992) when observing the breakdown of their model (essentially a numerical evaluation of (3.1)), outside the core of the vortex, in comparison to their experimental results. A numerical evaluation of (3.18), using an observed azimuthal velocity profile as initial field, shows that the extra Ekman pumping term does not significantly alter the previous results (even though $\epsilon = 0.45$). This has to be attributed to the smallness of the numerical factors preceding the added terms, alluded to in the Appendix. In fact, Kloosterziel & van Heijst remark that even for small values of the Rossby number their profiles deviate from those predicted by a linear analysis insofar as the velocity field at large radii drops at a faster rate than closer to the core of the vortex: a feature which the proposed extra Ekman pumping term is clearly unable to account for.

4. Vortex evolution due to free-surface effects ($\epsilon \ll 1$)

When the Rossby number is vanishingly small ($\epsilon \ll 1$) the decay of a concentrically located axisymmetric vortex, whose initial azimuthal velocity structure is given by $v_0(r)$, is determined by viscous effects near the bottom, modified by effects due to a free surface. Its evolution follows from (2.10), setting $\epsilon = 0$, together with (A 4) and is given by

$$2v = \frac{\partial \eta}{\partial r}, \qquad \frac{\partial v}{\partial t}+2u = 0, \tag{4.1a, b}$$

$$F\frac{\partial \eta}{\partial t}+\frac{1}{r}\frac{\partial}{\partial r}(ru(1+\tfrac{1}{2}Fr^2-z_0)) = \frac{1}{2r}\frac{\partial}{\partial r}(rv). \tag{4.1c}$$

The last equation shows that the Ekman pumping at the top of the bottom boundary layer (the right-hand-side term) does not only contribute to the meridional

circulation, but can partly be offset by a displacement of the free surface. These equations can be combined into one single equation for the elevation, η:

$$4F\frac{\partial\eta}{\partial t}-\frac{1}{r}\frac{\partial}{\partial r}\left(r\frac{\partial^2\eta}{\partial r\,\partial t}(1+\tfrac{1}{2}Fr^2-z_0)+r\frac{\partial\eta}{\partial r}\right)=0, \tag{4.2a}$$

or, for the azimuthal velocity, v:

$$4F\frac{\partial v}{\partial t}-\frac{\partial}{\partial r}\left(\frac{1}{r}\frac{\partial}{\partial r}\left(r\frac{\partial v}{\partial t}(1+\tfrac{1}{2}Fr^2-z_0)+rv\right)\right)=0. \tag{4.2b}$$

A clear physical interpretation of (4.2) is given by O'Donnell & Linden (1991), who interpret (4.2a) as an evolution equation of quasi-geostrophic vorticity, $\omega=(1/2r)\,(\partial/\partial r)\,(r\,\partial\eta/\partial r)$. Following these authors, rewriting (4.2a) as

$$(1+\tfrac{1}{2}Fr^2-z_0)\frac{\partial\omega}{\partial t}=-\omega+2F\frac{\partial\eta}{\partial t}+2u\frac{\partial}{\partial r}(\tfrac{1}{2}Fr^2-z_0) \tag{4.3}$$

shows that the decay of the vortex is induced by vortex compression due to Ekman pumping (or suction), free-surface variations, or advection by the meridional circulation; physical effects which correspond to the three terms on the right-hand side of (4.3) respectively. The choice of a parabolic bottom profile, $z_0=\frac{1}{2}Fr^2$, mimicking the free-surface parabola, clearly eliminates the last vortex stretching term. As discussed in O'Donnell & Linden (1991) in the context of solid-body spin-up in a flat-bottomed cylinder, spin-down near the axis (where the radial advection is absent) is delayed because the Ekman pumping is offset by the raising of the free surface. Even though these two effects cooperate near the tank wall, spin-down is again delayed since the combination of the two will now be offset by the advection and stretching of background vorticity. It turns out that the combined effect is constant, so that the fluid remains in solid-body motion: the delay factor is radially uniform and proportional to the Froude number, see figure 5(a). In contrast, when there is no background vorticity gradient, as when the bottom is parabolic, the spin-down near the tank wall is fast (i.e. having a nondimensional e-folding timescale $O(1)$), since the vortex compression, produced by Ekman pumping and descent of the free surface, is unmatched, whereas near the axis these two effects oppose each other and the spin-up will again be delayed by a factor proportional to the Froude number. In the latter case, therefore, spin-up is a more complicated function of radial position (Cederlöf 1988), see figure 5(b). The difference between both geometries in spin-down timescales at the tank wall also follows from a consideration of the boundary condition. Since the fluid, which is displaced during spin-down, conserves mass,

$$\int_0^R r\eta\,\mathrm{d}r=0, \tag{4.4}$$

the evolution of azimuthal velocity at the tank wall is a simple exponential in time. This follows by integrating r times (4.2a) over the tank radius, employing (4.1a) to eliminate the free-surface gradient and using the fact that the azimuthal velocity vanishes at the centre:

$$(1+\tfrac{1}{2}FR^2-z_0(R))\,\partial v/\partial t+v=0. \tag{4.5}$$

For a parabolic bottom the boundary condition is

$$v(R,t)=v_0(R)\,\mathrm{e}^{-t}, \tag{4.6}$$

whereas for a flat-bottomed cylinder

$$v(R,t)=v_0(R)\,\mathrm{e}^{-t/(1+\frac{1}{2}FR^2)}. \tag{4.7}$$

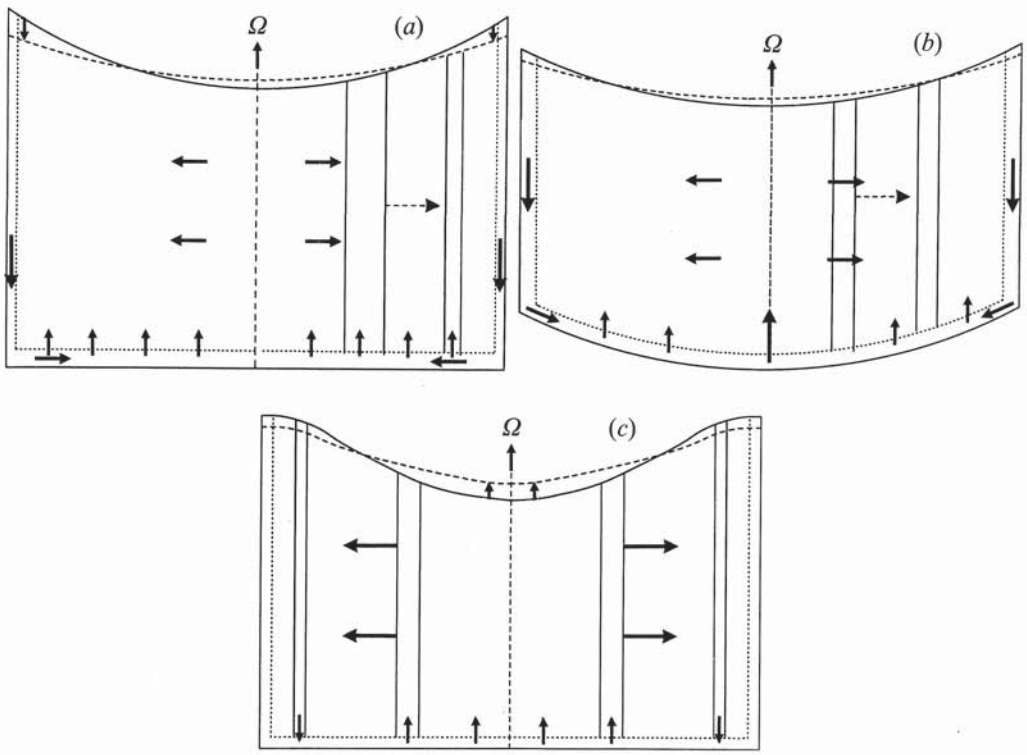

FIGURE 5. Sketch of free-surface effects in solid-body spin-down in (*a*) a flat-bottomed cylinder and (*b*) a cylinder with a parabolic bottom. In both cases, close to the rotation axis the stretching of the vortex tube due to Ekman pumping is offset by the raising of the free-surface (whose initial shape is denoted by a solid line). In the outer regions, however, the surface is descending and thus adds to the Ekman pumping. In (*a*) these two are offset by the stretching of background ('planetary') vortex tubes due to the (linear) radial outward flow. In (*b*) the background vorticity is uniform and thus does not counteract the two compressing mechanisms. Hence vorticity in these outer regions is quickly reduced and the spin-down of the outer region is relatively fast. (*c*) In a vortex the vorticity profile is non-uniform (see figure 4) and the previous picture is altered in the outer regions, where the vorticity is negative, which consequently leads to Ekman suction, rather than pumping.

Thus the decay factor for solid-body spin-down (for which $R = 1$, as in this case the tank radius is the only lengthscale involved) is increased by a factor $1+\frac{1}{2}F$. This is essentially the factor determined by Kloosterziel & van Heijst (1992) and O'Donnell & Linden (1991); the slight difference between our expression and theirs is due to the use of a different scaling.

Considering the spin-down of vortices, we can anticipate that the decay of the core, which is close to solid-body rotation, will be faster than in the more remote parts of the vortex, i.e. at distances beyond the radius where the azimuthal velocity profile has its maximum, as the Ekman pumping in these outer regions of the vortex will be small, due to the smallness of the vorticity of the overlying fluid. Also, since the azimuthal velocity has to satisfy (4.6) or (4.7) at the tank wall, the decay of a vortex in a parabolic basin will be relatively fast compared to that in a right-circular cylinder.

In the next two sections, we will consider the spin-down of a free-surface fluid in a parabolic and flat-bottomed tank respectively. In both cases it will be convenient

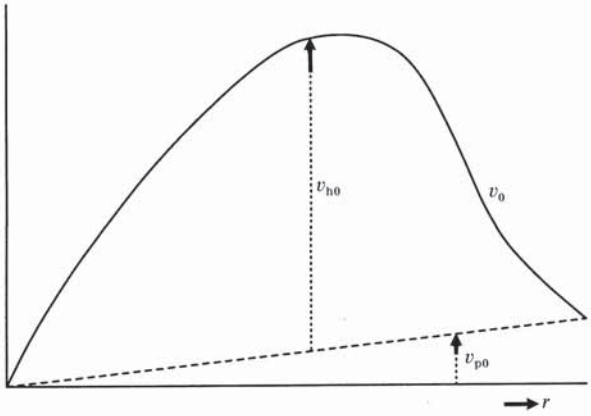

FIGURE 6. Separation of the initial azimuthal velocity profile into a particular part (which is linear with radius) and a homogeneous part (which vanishes at the tank wall).

to employ the linearity of the evolution equation, (4.2*b*), to split the solution into a particular, solid-body part, $v_p(r,t)$, having a linearly increasing azimuthal velocity which satisfies either (4.6), or (4.7) at the tank wall, and the homogeneous remainder, $v_h(r,t)$, whose azimuthal velocity has to vanish at the tank wall:

$$v_h(R,t) = 0. \tag{4.8}$$

4.1. *Vortex evolution in a parabolic basin*

When the bottom is parallel to the equilibrium parabolic shape of the free surface,

$$z_0(r) = \tfrac{1}{2}Fr^2,$$

up to some radius $r = R$, the evolution of a vortex with initial profile

$$v(r,0) = v_0(r)$$

is, from (4.2*b*), given by

$$4F\frac{\partial v}{\partial t} - \frac{\partial}{\partial r}\left(\frac{1}{r}\frac{\partial}{\partial r}\left(r\frac{\partial v}{\partial t} + rv\right)\right) = 0, \tag{4.9}$$

subject to the boundary condition (4.6) at $r = R$. The mathematical advantage of the present geometry is that (4.9) is separable, as was observed by Berman *et al.* (1983) for a two-layer fluid and Cederlöf (1988) for a homogeneous fluid. The temporal part is a simple exponential and the radial part is determined by a Bessel equation. The general solution, regular at the centre of the tank, therefore reads

$$v(r,t) = \sum_{n=1}^{\infty} A_n J_1(j_n r/R)\, \mathrm{e}^{S_n t}, \tag{4.10a}$$

with

$$S_n = -j_n^2/(j_n^2 + 4FR^2), \tag{4.10b}$$

where $J_1(x)$ denotes a first-order Bessel function of the first kind and j_n are the successive zeros of $J_1(x)$. The Froude number FR^2 appearing in (4.10*b*), which determines the decay rate of the constituting eigenmodes, is based solely on the tank radius and is thus independent of the vortex size. The initial velocity field is split in a solid-body part and a homogeneous part, which satisfies (4.8), as discussed above (see figure 6):

$$v_0(r) = v_{p0}(r) + v_{h0}(r),$$

with $$v_{\mathrm{p}0}(r) = rv_0(R)/R, \quad v_{\mathrm{h}0}(r) = v_0(r) - v_{\mathrm{p}0}(r). \tag{4.11}$$

The Bessel functions $J_1(j_n r/R)$, with weight function r, form a complete set on the interval $0 \leqslant r \leqslant R$. The undetermined coefficients A_n of the Fourier–Bessel expansion (4.10) therefore follow from a projection of the initial profile on each of these eigenfunctions (Carslaw & Jaeger 1959, p. 196). The resulting solution thus reads

$$v(r,t) = v_{\mathrm{p}}(r,t) + v_{\mathrm{h}}(r,t), \tag{4.12a}$$

with $$v_{\mathrm{p}}(r,t) = v_{\mathrm{p}0}(r)\left(\mathrm{e}^{-t} - 2\frac{R}{r}\sum_{n=1}^{\infty}\frac{J_1(j_n r/R)}{j_n J_0(j_n)}(\mathrm{e}^{S_n t} - \mathrm{e}^{-t})\right), \tag{4.12b}$$

and $$v_{\mathrm{h}}(r,t) = \frac{2}{R^2}\sum_{n=1}^{\infty}\frac{1}{J_0^2(j_n)}\int_0^R s v_{\mathrm{h}0}(s)\, J_1(j_n s/R)\,\mathrm{d}s\, J_1(j_n r/R)\,\mathrm{e}^{S_n t}. \tag{4.12c}$$

The particular part is related to Cederlöf's (1988) solution, who calculated the free-surface shape during a solid-body spin-up process. Note that the first and third terms in (4.12*b*), i.e. those proportional to e^{-t}, in fact cancel (Prudnikov, Brychkov & Marichev 1986, p. 690, in combination with the recurrence relation of the Bessel functions). The remaining series related to the second term, however, when truncated at a certain $n = N$, displays the Gibb's phenomenon at the tank wall; a feature from which the form presented in (4.12*b*) is free.

Example: the Rankine vortex

As an example we consider the Rankine vortex, whose initial profile is given by (3.6), for which the evolution can be determined explicitly. For more realistic vortex profiles, the integral in (4.12*c*) has to be evaluated numerically. Inserting (3.6) into (4.11) yields the following initial profiles for the particular and homogeneous parts respectively:

$$v_{\mathrm{p}0}(r) = r/R^2, \tag{4.13a}$$

$$v_{\mathrm{h}0}(r) = \begin{cases} r(1-1/R^2), & r \leqslant 1, \\ 1/r - r/R^2, & 1 \leqslant r \leqslant R. \end{cases} \tag{4.13b}$$

Thus the evolving particular and homogeneous parts can be obtained from (4.12) and read

$$v_{\mathrm{p}}(r,t) = \frac{1}{R}\left(\frac{r}{R}\,\mathrm{e}^{-t} - 2\sum_{n=1}^{\infty}\frac{J_1(j_n r/R)}{j_n J_0(j_n)}(\mathrm{e}^{S_n t} - \mathrm{e}^{-t})\right), \tag{4.14a}$$

$$v_{\mathrm{h}}(r,t) = 4\sum_{n=1}^{\infty}\frac{J_1(j_n/R)}{j_n^2 J_0^2(j_n)}J_1(j_n r/R)\,\mathrm{e}^{S_n t}, \tag{4.14b}$$

in which $J_0(x)$ denotes the zeroth-order Bessel function of the first kind. In most compact form this can be combined as

$$v(r,t) = 2\sum_{n=1}^{\infty}\frac{J_1(j_n r/R)}{j_n^2 J_0^2(j_n)}\left(2J_1(j_n/R) - \frac{j_n}{R}J_0(j_n)\right)\mathrm{e}^{S_n t},$$

but a truncated form of this does again show the Gibb's phenomenon, absent in the addition of (4.14*a*) and (4.14*b*), though not in its truncated spectral vorticity representation. Figure 7 shows the decaying Rankine vortex at a few instances.

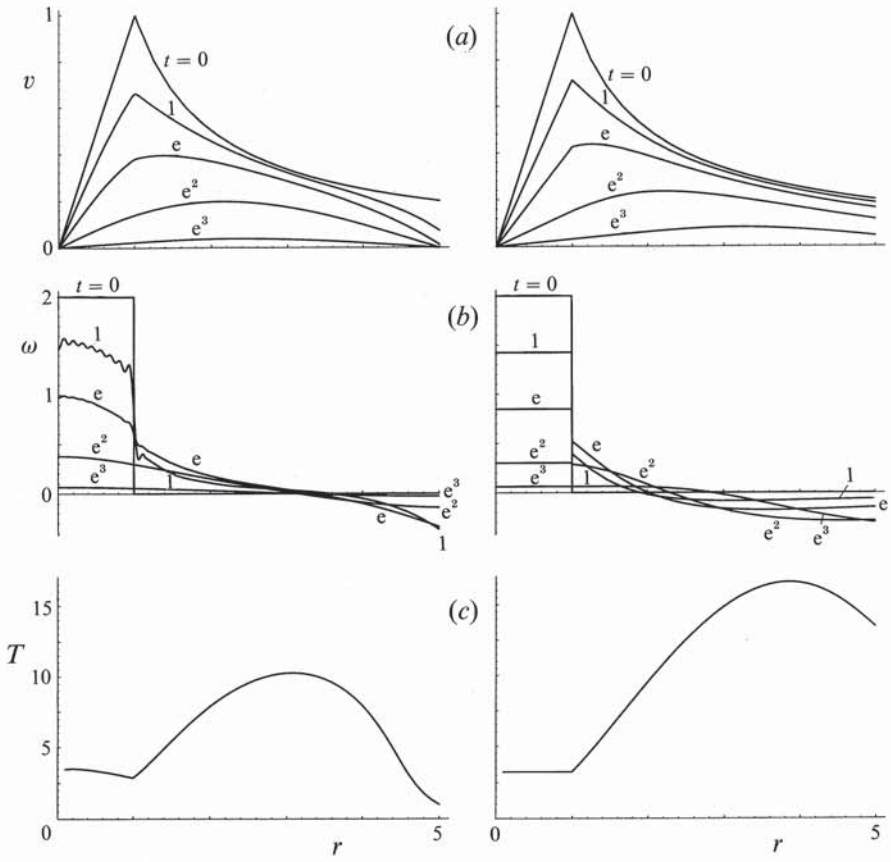

FIGURE 7. Free-surface effects on the spin-down of a cyclonic Rankine vortex in a cylinder having a parabolic bottom (left) and a right-circular cylinder (right). Azimuthal velocity (*a*) and vorticity (*b*) profiles (for successive instances of time, t) and decay-time (*c*) as a function of radius. Note that the wiggles in the vorticity profile of the Rankine vortex (and in the decay time for small radii) in a parabolic basin are due to truncation of the infinite series.

As remarked, from a geophysical point of view the use of a cylinder with a parabolic bottom is attractive since its background vorticity is uniform. The evolution of a vortex in such a basin, under the influence of a free surface, may therefore model the evolution of f-plane vortices more closely than those in the flat-bottomed cylinder. When the vortex scale is much less than the tank radius (such that the dimensionless tank radius R approaches infinity) the Fourier–Bessel expansion turns into a Fourier–Bessel integral. The particular part of the azimuthal velocity field vanishes in this case and the vortex profile, following from (4.12*c*) by a limiting procedure (Nikiforov & Uvarov 1988, p. 316), evolves as

$$v(r,t) = \int_0^\infty k\hat{v}_0(k)\, J_1(kr) \exp\left(\frac{-k^2 t}{k^2+4F}\right) \mathrm{d}k, \tag{4.15a}$$

where $\hat{v}_0(k)$ is the Fourier–Bessel transform of the initial azimuthal velocity field,

$$\hat{v}(k) = \int_0^\infty r v_0(r)\, J_1(kr)\, \mathrm{d}k. \tag{4.15b}$$

From (4.1a) the elevation field then evolves as

$$\eta(r,t) = \int_0^\infty \hat{\eta}_0(k)\, J_0(kr) \exp\left(\frac{-k^2 t}{k^2+4F}\right) \mathrm{d}k, \tag{4.15c}$$

with

$$\hat{\eta}_0(k) = \int_0^\infty \eta_0(r)\, J_0(kr)\, \mathrm{d}r. \tag{4.15d}$$

Even though vortices in the ocean are often damped by lateral friction (Mied 1989), there are circumstances where bottom or surface (when covered with sea ice) friction is dominant. The latter applies to the eddies in the Weddell Sea as Ou & Gordon (1986) have shown. Except for the entrainment which they included the eddy evolves as in (4.15) and in particular the decay time increases with increasing Froude number. As in the decay of a fluid which initially is in solid-body rotation (Cederlöf 1988) this decay time is a function of radius: the decay is relatively fast at the outer edge and in the core, but slower in between (see figure 7c).

4.2. *Vortex evolution in a flat-bottomed cylinder*

When the bottom of the cylinder is flat, $z_0(r) = 0$, the evolution of a vortex with initial profile

$$v(r,0) = v_0(r)$$

is, from (4.2b) given by

$$4F\frac{\partial v}{\partial t} - \frac{\partial}{\partial r}\left(\frac{1}{r}\frac{\partial}{\partial r}\left(r\frac{\partial v}{\partial t}(1+\tfrac{1}{2}Fr^2)+rv\right)\right) = 0, \tag{4.16}$$

subject to boundary condition (4.5):

$$(1+\tfrac{1}{2}FR^2)\,\partial v/\partial t + v = 0 \quad \text{at} \quad r = R, \tag{4.17}$$

and a requirement that $v(r,t)$ vanishes at the centre of the tank. Introducing the angular velocity

$$\Omega = v/r \tag{4.18a}$$

and the radial coordinate

$$s = \tfrac{1}{2}Fr^2 \tag{4.18b}$$

into (4.16–4.17) yields

$$2\frac{\partial \Omega}{\partial t} - \frac{\partial^2}{\partial s^2}\left(s\frac{\partial \Omega}{\partial t}(1+s)+s\Omega\right) = 0, \tag{4.19a}$$

and the boundary condition

$$(1+S)\,\partial\Omega/\partial t + \Omega = 0 \quad \text{at} \quad s = S, \tag{4.19b}$$

where

$$S = \tfrac{1}{2}FR^2. \tag{4.20}$$

At the origin we require Ω to be finite:

$$\Omega < \infty \quad \text{at} \quad s = 0. \tag{4.21}$$

The only place where the Froude number enters is via the position of the boundary, $s = S$. Since two of the terms in (4.19a) cancel, this equation can be written as

$$\left((1+s)\frac{\partial}{\partial t}+1\right)\left(s\frac{\partial^2 \Omega}{\partial s^2}+2\frac{\partial \Omega}{\partial s}\right)+2s\frac{\partial^2 \Omega}{\partial s\,\partial t} = 0. \tag{4.22}$$

In particular (4.22) is satisfied by any s-independent angular velocity of arbitrary temporal behaviour; a degree of freedom which we use to simplify the boundary condition at the tank wall by writing Ω as the sum of a particular part, $\Omega_{\rm p}$, satisfying (4.19b):

$$\Omega_{\rm p}(s,t) = \Omega_{\rm p0}(S)\,{\rm e}^{-t/(1+S)}, \tag{4.23}$$

and a homogeneous part, $\Omega_{\rm h}$, satisfying (4.22), but vanishing at the tank wall. The particular solution, (4.23), corresponding to a solid-body motion of the fluid, was previously obtained by Kloosterziel & van Heijst (1992) and O'Donnell & Linden (1991). In the latter study, the increased spin-up timescale, determined by the denominator of the exponent in (4.23), has been carefully verified in a number of laboratory experiments.

The evolution of the remaining initial part of the angular velocity profile:

$$\Omega_{\rm h}(s,0) \equiv \Omega_{\rm h0}(s) = \Omega_0(s) - \Omega_{\rm p0}(s),$$

is determined by the general solution of (4.22). This is obtained by multiplying this equation by s and introducing the auxiliary variable

$$h \equiv s^2\,\partial\Omega_{\rm h}/\partial s, \tag{4.24}$$

leaving

$$\left((1+s)\frac{\partial}{\partial t}+1\right)\frac{\partial h}{\partial s}+2\frac{\partial h}{\partial t}=0. \tag{4.25}$$

With the new radial coordinate

$$\xi = 1+s, \tag{4.26}$$

this becomes

$$\left(\xi\frac{\partial}{\partial t}+1\right)\frac{\partial h}{\partial \xi}+2\frac{\partial h}{\partial t}=0,$$

or, equivalently,

$$\left(\xi\frac{\partial}{\partial \xi}+2\right)\frac{\partial h}{\partial t}+\frac{\partial h}{\partial \xi}=0.$$

Putting

$$h = \partial w/\partial \xi, \tag{4.27}$$

we observe that the equation can finally be contracted to

$$\frac{\partial^2}{\partial \xi^2}\left(\xi\frac{\partial w}{\partial t}+w\right)=0. \tag{4.28}$$

The general solution of this equation is given by

$$w = W(\xi)\,{\rm e}^{-t/\xi}+\int_0^t a(\tau)\,{\rm e}^{(\tau-t)/\xi}\,{\rm d}\tau+\frac{1}{\xi}\int_0^t b(\tau)\,{\rm e}^{(\tau-t)/\xi}\,{\rm d}\tau, \tag{4.29}$$

where $W(\xi)$, $a(\tau)$ and $b(\tau)$ are arbitrary functions, to be determined by the boundary and initial conditions. As remarked in Myint-U & Debnath (1987, p. 3) 'the selection of a particular solution satisfying the supplementary conditions from the general solution of a partial differential equation may be as difficult as, or even more difficult than the problem of finding the general solution, because the general solution involves arbitrary functions'. In the present problem we can simply dispense with the functions $a(\tau)$ and $b(\tau)$ (by setting them equal to zero) in view of the simple form of the boundary condition. The remaining degree of freedom, $W(\xi)$ – which, expressed in the related radial coordinate s, is denoted as $w_0(s)$ – as well as the solution, $\Omega_{\rm h}(s,t)$

itself are entirely determined by the initial profile $\Omega_{\mathrm{h}0}(s)$. From (4.24), (4.26) and (4.27) we obtain

$$\frac{\partial \Omega_{\mathrm{h}}}{\partial s} = \frac{1}{s^2}\frac{\partial w}{\partial s}, \tag{4.30}$$

a diagnostic relation that can be used 'both ways'; i.e. given the initial profile of the angular velocity, $\Omega_{\mathrm{h}0}(s)$, we may determine $w_0(s)$ from it:

$$w_0(s) = \int_0^s \sigma^2 \frac{\partial \Omega_{\mathrm{h}0}}{\partial \sigma}\,\mathrm{d}\sigma + w_0(0). \tag{4.31}$$

By a partial integration and setting $w_0(0) = 0$ to ensure regularity of $w_0(s)/s^2$ – a condition whose necessity follows from the required regularity of Ω_{h} at $s = 0$; see (4.33) below – this can be written as

$$w_0(s) = s^2\left(\Omega_{\mathrm{h}0}(s) - \int_0^1 \Omega_{\mathrm{h}0}(s\zeta^{\frac{1}{2}})\,\mathrm{d}\zeta\right). \tag{4.32}$$

Conversely, (4.30) also provides us with the general solution, $\Omega_{\mathrm{h}}(s,t)$, at an arbitrary time. By integrating (4.30) from an interior value s to the boundary S we obtain, employing the fact that the angular velocity vanishes at the tank wall,

$$\Omega_{\mathrm{h}}(s,t) = -\int_s^S \frac{1}{\sigma^2}\frac{\partial w}{\partial \sigma}\,\mathrm{d}\sigma = \frac{w(s,t)}{s^2} - \frac{w(S,t)}{S^2} - 2\int_s^S \frac{w}{\sigma^3}\,\mathrm{d}\sigma. \tag{4.33}$$

Inserting the restricted solution (4.29), expressed in terms of s,

$$w(s,t) = w_0(s)\,\mathrm{e}^{-t/(1+s)}, \tag{4.34}$$

with the initial field $w_0(s)$ given by (4.32), into (4.33) finally yields

$$\begin{aligned}\Omega_{\mathrm{h}}(s,t) = \Omega_{\mathrm{h}0}(s)\,\mathrm{e}^{-t/(1+s)} &+ \int_0^1 (\Omega_{\mathrm{h}0}(S\zeta^{\frac{1}{2}})\,\mathrm{e}^{-t/(1+S)} - \Omega_{\mathrm{h}0}(s\zeta^{\frac{1}{2}})\,\mathrm{e}^{-t/(1+s)})\,\mathrm{d}\zeta \\ &- 2\int_s^S \frac{1}{\sigma}\left(\Omega_{\mathrm{h}0}(\sigma) - \int_0^1 \Omega_{\mathrm{h}0}(\sigma\zeta^{\frac{1}{2}})\,\mathrm{d}\zeta\right)\mathrm{e}^{-t/(1+\sigma)}\,\mathrm{d}\sigma,\end{aligned} \tag{4.35}$$

where we have used the fact that $\Omega_{\mathrm{h}0}(S) = 0$. One may check that the angular velocity satisfies (4.22), vanishes identically at the tank wall, remains finite at the centre and is equal to the initial profile by construction. Note the highly convoluted way in which the initial angular velocity profile, $\Omega_{\mathrm{h}0}(s)$, appears in the final expression of the angular velocity at a specific time t and 'radius' s.

The azimuthal velocity profile itself is, as in (4.12*a*), given by the sum of the particular and homogeneous velocity fields that follow from a multiplication of (4.23) and (4.35) by r, and replacing the introduced variables s and S with the aid of (4.18*b*) and (4.20).

Example: the Rankine vortex

It is again useful to consider the Rankine vortex, split into the solid-body and remaining parts, (4.13). The initial profile of the variable w is determined by (4.32) and, for this case, given by

$$w_0(s) = \begin{cases} 0, & s \leqslant \frac{1}{2}F, \\ \frac{1}{2}F(\frac{1}{2}F - s), & \frac{1}{2}F \leqslant s \leqslant S. \end{cases} \tag{4.36}$$

With this initial profile the azimuthal velocity structure as a function of time is given as

$$v(r,t) = r(\Omega_{\rm h}(r,t) + (1/R^2)\,\mathrm{e}^{-t/(1+\frac{1}{2}FR^2)}), \tag{4.37a}$$

where the homogeneous angular velocity profile is given by

$$\Omega_{\rm h}(r,t) = \Omega_1\,\mathrm{e}^{-t/(1+\frac{1}{2}Fr^2)} + \Omega_2\,\mathrm{e}^{-t/(1+\frac{1}{2}FR^2)} - 2\,\mathrm{e}^{-t}\left[\left(\frac{1+a\tau}{2a} - \left(1+\frac{F}{2}\right)\right)\frac{\mathrm{e}^{a\tau}}{a}\right.$$
$$\left. - \left(\frac{1+b\tau}{2b} - \left(1+\frac{F}{2}\right)\right)\frac{\mathrm{e}^{b\tau}}{b} + \left(\frac{\tau^2}{2} - \tau\left(1+\frac{F}{2}\right)\right)(\mathrm{Ei}(b\tau) - \mathrm{Ei}(a\tau))\right], \tag{4.37b}$$

in which the following piecewise-defined (but continuous) functions appear:

$$\Omega_1 = \begin{cases} 0, & r \leqslant 1, \\ \dfrac{1}{r^2}\left(\dfrac{1}{r^2} - 1\right), & 1 \leqslant r \leqslant R, \end{cases} \qquad a = \begin{cases} \dfrac{1}{1+\frac{1}{2}F}, & r \leqslant 1, \\ \dfrac{r^2}{1+\frac{1}{2}Fr^2}, & 1 \leqslant r \leqslant R. \end{cases} \tag{4.37c, d}$$

The remaining variables are defined as

$$\Omega_2 = \frac{1}{R^2}\left(1 - \frac{1}{R^2}\right), \quad b = \frac{R^2}{1+\frac{1}{2}FR^2}, \quad \tau = \frac{F}{2}t. \tag{4.37e}$$

The function $\mathrm{Ei}(x)$ in (4.37*b*) denotes the exponential integral. Note that the core of the Rankine vortex remains in solid-body rotation; nevertheless the velocity profile manages to become continuous and spread outwards (see figure 7). In comparison to the decay of a Rankine vortex in a cylinder with a parabolic bottom, the left-hand side of figure 7, it is clear that the decay in a flat-bottomed cylinder is prolonged by the presence of a background vorticity gradient. This is due to the production of negative relative vorticity in the outer region of the vortex by outward advection of low-vorticity fluid in addition to the production of this by the descending free surface. Only the latter mechanism was also present in the parabolic basin.

The evolution of other initial profiles cannot usually be described in terms of special functions and have to be obtained by integrating the expressions in (4.35) numerically.

5. Conclusions

The decay of a barotropic axisymmetric vortex in a rapidly rotating ($E^{\frac{1}{2}} \ll 1$) cylinder of moderate aspect ratio ($\delta = H/L \leqslant O(1)$) is due to bottom friction. In the classical case, in which both nonlinear and free-surface effects are absent ($\epsilon = F = 0$), this decay due to Ekman pumping is self-similar, has the position of the peak of the azimuthal velocity profile fixed and has a decay time given by the Ekman timescale $T_E = \Omega_0^{-1} E^{-\frac{1}{2}}$ (Greenspan & Howard 1963). In regions where the relative vorticity of the fluid is positive (negative), friction in the bottom layer will lead to Ekman pumping (suction) at the top of this layer, hence compressing (stretching) vortex tubes in the interior, and by conservation of potential vorticity will reduce (increase) the vorticity in the fluid, thus bringing it closer to the background vorticity.

When the Rossby number is not small ($\epsilon \neq 0$) nonlinear advection of relative vorticity by the radial Ekman flow in the interior will cause the position of the peak in the azimuthal velocity profile to propagate outwards or inwards for cyclonic and

anticyclonic vortices respectively. Since the propagation speed is proportional to the strength of the azimuthal velocity this in turn will lead to a steepening of the azimuthal velocity profile in the radial direction. Indeed when the absolute vorticity of the initial profile is negative somewhere, this profile will develop into a shock within a finite time. This discontinuity in azimuthal velocity will in reality be smoothed out by viscous diffusion (neglected here) and, when the scale of the shock is much smaller than the radius at which the shock appears, can be described by Burgers' equation (as in Venezian 1970). For anticyclonic vortices having a monotonically increasing angular velocity profile this shock will always develop at the core of the vortex. The dynamical condition at which multivaluedness starts to appear is, surprisingly, virtually equivalent to Rayleigh's (1916) kinematical criterion, despite significant differences in the physical mechanisms involved.

When the free surface is dynamically active, as when the Froude number is not small ($F \neq 0$), the peak in the azimuthal velocity structure is similarly observed to propagate outwards, except that the total profile spreads out. This and the related increase in decay time (with proportionality factor related to the Froude number) are due to the ability of the free surface to partially offset the compression (and stretching) of vortex columns in the positive (negative) vorticity regions of the vortex. The relatively fast decay of a vortex in a cylinder having a parabolic bottom as compared to one which is flat bottomed is because the decay factor at the tank wall is proportional to the depth of the fluid at the wall, which is obviously larger in the latter case (assuming that the central depth is the same in both cases).

The author acknowledges the great benefit that he obtained from discussions on the subject treated in this paper with Ruud Kloosterziel, Gert-Jan van Heijst, Ulf Cederlöf, Huib de Swart and Sjef Zimmerman. He is also grateful to Herman Ridderinkhof for help with numerical computations and to a referee for his comments on the physical interpretation of the breaking criterion.

Appendix. The Ekman pumping velocity

Near the bottom viscous effects require the velocity to decrease to zero quickly and, correspondingly, the vertical scale is set by the Ekman scale $HE^{\frac{1}{2}}$ rather than by the total depth, H. In this boundary layer an $O(U)$ change, which the azimuthal velocity field experiences when brought from its inviscid value in the 'interior' region towards zero at the bottom, produces an $O(U)$ change in the radial velocity field (due to the Coriolis force), which is thus not small any longer, as it was in the interior. The non-dimensional equations expressing the dynamics in the boundary layer therefore follow from (2.5) by a subsequent rescaling: $[u, z] \rightarrow [E^{-\frac{1}{2}}u, E^{\frac{1}{2}}z]$. Setting $E = 0$ again in the resulting equations shows that the pressure field remains hydrostatic and the pressure gradient is thus given by its value at 'infinity', i.e. in the interior:

$$\partial p'/\partial r = \epsilon v_\infty^2/r + 2v_\infty. \tag{A 1}$$

Also, the time-derivative terms drop out, such that the evolution of the boundary-layer field is entirely determined by (slaved to) the evolving azimuthal velocity field, $v_\infty(r;t)$. The resulting boundary-layer equations in this rotating frame of reference are thus given by

$$\epsilon\left(u\frac{\partial u}{\partial r} + w\frac{\partial u}{\partial z} - \frac{v^2}{r}\right) - 2v + \epsilon\frac{v_\infty^2}{r} + 2v_\infty = \frac{\partial^2 u}{\partial z^2}, \tag{A 2a}$$

$$\epsilon\left(u\frac{\partial v}{\partial r}+w\frac{\partial v}{\partial z}+\frac{uv}{r}\right)+2u=\frac{\partial^2 v}{\partial z^2},\quad \frac{\partial w}{\partial z}+\frac{1}{r}\frac{\partial}{\partial r}(ru)=0, \tag{A 2b, c}$$

which, using the variables

$$\chi\equiv\frac{u+\mathrm{i}v}{r}\equiv-\frac{1}{2}\frac{\partial\phi}{\partial z}+\mathrm{i}\Omega,\quad w=\phi+\frac{\partial\phi}{\partial\xi},\quad \xi=\ln(r^2),\quad \Omega_\infty(\xi;t)=\frac{v_\infty(r;t)}{r},$$

can be expressed concisely as

$$\epsilon(J(\phi,\chi)+\phi\,\partial\chi/\partial z+\chi^2+\Omega_\infty^2)+2\,\mathrm{i}\chi+\Omega_\infty)=\partial^2\chi/\partial z^2, \tag{A 3}$$

where the Jacobian $J(\phi,\chi)\equiv(\partial\phi/\partial\xi)(\partial\chi/\partial z)-(\partial\chi/\partial\xi)(\partial\phi/\partial z)$. By continuity the radial boundary-layer flow produces a non-zero vertical flow far away from the boundary: the Ekman pumping – or suction velocity, w_E, whose determination in terms of the prescribed interior azimuthal velocity field forms the ultimate goal of the boundary-layer analysis.

An analytic solution to (A 3), subject to the boundary conditions

$$\chi=\phi=0\quad\text{at}\quad z=0$$

and

$$\chi\to\mathrm{i}\Omega_\infty\quad\text{as}\quad z\to\infty,$$

for arbitrary interior profiles, $\Omega_\infty(\xi;t)$ and arbitrary Rossby numbers, ϵ, is not known. For small values of the Rossby number, $|\epsilon|\ll 1$, however, (A 3) linearizes and we retrieve the familiar Ekman equations, whose Ekman pumping velocity is given by:

$$w_E^{(0)}=\frac{1}{2r}\frac{\partial}{\partial r}(r^2\Omega_\infty)=\frac{1}{2r}\frac{\partial}{\partial r}(rv_\infty)\equiv\tfrac{1}{2}\omega_\infty. \tag{A 4}$$

The dimensionless Ekman pumping velocity is therefore equal to half the dimensionless vorticity of the fluid directly overlying it. A regular perturbation expansion in the Rossby number, ϵ, yields its first-order correction, which reads

$$w_E^{(1)}=-\frac{1}{10r}\frac{\partial}{\partial r}\left(r^2\left(\Omega_\infty^2+\tfrac{7}{8}r\Omega_\infty\frac{\partial\Omega_\infty}{\partial r}\right)\right)=-\frac{1}{80r}\frac{\partial}{\partial r}\left(r\left(\frac{v_\infty^2}{r}+\frac{7}{2}\frac{\partial v_\infty^2}{\partial r}\right)\right). \tag{A 5}$$

As is obvious from (A 3) the Jacobian term vanishes identically in the case of solid-body spin-up, or spin-down, as Ω_∞ is then independent of ξ and so will Ω and ϕ be: we retrieve von Kármán's (1921) similarity equations. In this circumstance, which can only occur over an infinitely large disk, the Rossby number has its usual meaning in this context, as the ratio of the angular velocity of the fluid 'infinitely' far above (and relative to) the disk and the angular velocity of the disk: $\epsilon=(\Omega_\infty-\Omega_0)/\Omega_0$. The Ekman pumping velocities (and boundary-layer structure) for this idealized case have been computed by many authors (see Greenspan 1968) for arbitrary values of the above-defined Rossby number. It turns out that, for certain parameter ranges, the stationary state is not unique (as different inviscid cells, separated by viscous interlayers, may develop), or does not even exist (Zandbergen & Dijkstra 1987).

The relationship between Ekman pumping and angular velocity at infinity for the single-cell case was determined numerically by Rogers & Lance (1960). The linear relationship, (A 4), was thus observed to apply over a large range of Rossby numbers ($|\epsilon|<0.6$). Wedemeyer (1964), studying spin-up from rest in a finite cylinder, extended this linear relationship to apply over the entire range of interest ($-1\leqslant\epsilon\leqslant 0$) and his analytical results compared fairly well with the actually

observed evolving azimuthal velocity field in the interior, despite the facts that the spin-up took place in a finite cylinder and that the velocity profiles were not self-similar during the spin-up process, as the idealization of (A 3) to von Kármán's similarity theory presumes. Weidman (1976) took a best-fit curve to the numerically determined relationship between the Ekman pumping velocity and the Rossby number of Rogers & Lance (1960), which included the non-monotonic relation between the two for Rossby numbers slightly above $\epsilon = -1$. The exact solutions using this parametrization were, however, shown to be of dubious physical content (Benton 1979) as the vorticity, during the spin-up process, showed an unphysical maximum at an intermediate radial position. Evidently, an evaluation of (A 3) in response to a non-solid-body interior velocity field, with the vorticity stretching Jacobian term included, is required. The perturbation approach, as given by (A 5), can only be a first step in this process, even though it seems that (A 5) may also be valid for relatively large values of the Ekman number in view of the convergence provided by the numerical smallness of the coefficients leading the higher-order approximations.

When the bottom is sloping the Ekman pumping velocity is modified by a geometric factor (Greenspan 1968). Like Cederlöf (1988), we shall assume that the parameter which measures this modification, δF, is small, allowing the use of (A 4) directly (for small Rossby numbers).

REFERENCES

Benton, E. R. 1979 Vorticity dynamics in spin-up from rest. *Phys. Fluids* **22**, 1250–1251.

Benton, E. R. & Clark, A. 1974 Spin-up. *Ann. Rev. Fluid Mech.* **6**, 257–280.

Berman, A. S., Bradford, J. & Lundgren, T. S. 1983 Two-fluid spin-up in a centrifuge. *J. Fluid Mech.* **84**, 411–431.

Carslaw, H. S. & Jaeger, J. C. 1959 *Conduction of Heat in Solids.* Clarendon.

Carton, X. J. & McWilliams, J. C. 1989 Barotropic and baroclinic instabilities of axisymmetric vortices in a quasi-geostrophic model. In *Mesoscale/Synoptic Coherent Structures in Geophysical Turbulence* (ed. J. C. J. Nihoul & B. M. Jamart), pp. 225–244. Elsevier.

Cederlöf, U. 1988 Free-surface effects on spin-up. *J. Fluid Mech.* **187**, 395–407.

Chandrasekhar, S. 1961 *Hydrodynamic and Hydromagnetic Stability.* Clarendon.

Goller, H. & Ranov, T. 1968 Unsteady rotating flow in a cylinder with a free surface. *Trans. ASME* D: *J. Basic Engng* **90**, 445–454.

Greenspan, H. P. 1968 *The Theory of Rotating Fluids.* Cambridge University Press.

Greenspan, H. P. & Howard, L. N. 1963 On a time-dependent motion of a rotating fluid. *J. Fluid Mech.* **17**, 385–404.

Heijst, G. J. F. van & Kloosterziel, R. C. 1989 Tripolar vortices in a rotating fluid. *Nature* **338**, 569–571.

Heijst, G. J. F. van, Kloosterziel, R. C. & Williams, C. W. M. 1991 Laboratory experiments on the tripolar vortex in a rotating fluid. *J. Fluid Mech.* **225**, 301–331.

Kármán, T. von 1921 Über laminäre und turbulente Reibung. *Z. Angew. Math. Mech.* **1**, 233–252.

Kloosterziel, R. C. 1990 Barotropic vortices in a rotating fluid. Ph.D. thesis, University of Utrecht.

Kloosterziel, R. C. & Heijst, G. J. F. van 1989 On tripolar vortices. In *Mesoscale/Synoptic Coherent Structures in Geophysical Turbulence* (ed. J. C. J. Nihoul & B. M. Jamart), pp. 609–625. Elsevier.

Kloosterziel, R. C. & Heijst, G. J. F. van 1991 An experimental study of unstable barotropic vortices in a rotating fluid. *J. Fluid Mech.* **223**, 1–24.

Kloosterziel, R. C. & Heijst, G. J. F. van 1992 The evolution of stable barotropic vortices in a rotating free-surface fluid. *J. Fluid Mech.* **239**, 607–629.

MELANDER, M. V., MCWILLIAMS, J. C. & ZABUSKY, N. J. 1987 Axisymmetrization and vorticity-gradient intensification of an isolated two-dimensional vortex through filamentation. *J. Fluid Mech.* **178**, 137–159.

MICHALKE, A. & TIMME, A. 1967 On the inviscid instability of certain two-dimensional vortex-type flows. *J. Fluid Mech.* **29**, 647–666.

MIED, R. P. 1989 The decay of mesoscale vortices. In *Mesoscale/Synoptic Coherent Structures in Geophysical Turbulence* (ed. J. C. J. Nihoul & B. M. Jamart), pp. 135–147. Elsevier.

MYINT-U, Y. & DEBNATH, L. 1987 *Partial Differential Equations for Scientists and Engineers.* North-Holland.

NIKIFOROV, A. F. & UVAROV, V. B. 1988 *Special Functions of Mathematical Physics.* Birkhäuser.

O'DONNELL, J. & LINDEN, P. F. 1991 Free-surface effects on the spin-up of fluid in a rotating cylinder. *J. Fluid Mech.* **232**, 439–453.

OU, H. W. & GORDON, A. L. 1986 Spin-down of baroclinic eddies under sea-ice. *J. Geophys. Res.* **91**, 7623–7630.

PRUDNIKOV, A. P., BRYCHKOV, YU. A. & MARICHEV, O. I. 1986 *Integrals and Series*, Vol. 2. Gordon and Breach.

RAYLEIGH, LORD 1916 On the dynamics of revolving fluids. *Proc. R. Soc. Lond.* A **93**, 148–154.

ROGERS, M. H. & LANCE, G. N. 1960 The rotationally symmetric flow of a viscous fluid in the presence of an infinite rotating disk. *J. Fluid Mech.* **7**, 617–631.

SAFFMAN, P. G. & BAKER, G. R. 1979 Vortex interactions. *Ann. Rev. Fluid Mech.* **11**, 95–122.

VENEZIAN, G. 1970 Nonlinear spin-up. *Topics in Ocean Engineering*, Vol. 2, pp. 87–96. Gulf Publishing Co.

WATKINS, W. B. & HUSSEY, R. G. 1977 Spin-up from rest in a cylinder. *Phys. Fluids* **20**, 1596–1604.

WEDEMEYER, E. H. 1964 The unsteady flow within a spinning cylinder. *J. Fluid Mech.* **20**, 383–399.

WEIDMAN, P. D. 1976 On the spin-up and spin-down of a rotating fluid. Part 1. Extending the Wedemeyer model. *J. Fluid Mech.* **77**, 658–708.

WHITHAM, G. B. 1974 *Linear and Nonlinear Waves.* Wiley-Interscience.

ZANDBERGEN, P. J. & DIJKSTRA, D. 1987 Von Kármán swirling flows. *Ann. Rev. Fluid Mech.* **19**, 465–491.